

## Small-scale variation in ecosystem CO<sub>2</sub> fluxes in an alpine meadow depends on plant biomass and species richness

Mitsuru Hirota · Pengcheng Zhang · Song Gu ·  
Haihua Shen · Takeo Kuriyama · Yingnian Li ·  
Yanhong Tang

Received: 23 August 2009 / Accepted: 21 December 2009 / Published online: 25 February 2010  
© The Botanical Society of Japan and Springer 2010

**Abstract** Characterizing the spatial variation in the CO<sub>2</sub> flux at both large and small scales is essential for precise estimation of an ecosystem's CO<sub>2</sub> sink strength. However, little is known about small-scale CO<sub>2</sub> flux variations in an ecosystem. We explored these variations in a *Kobresia* meadow ecosystem on the Qinghai-Tibetan plateau in relation to spatial variability in species composition and biomass. We established 14 points and measured net ecosystem production (NEP), gross primary production (GPP), and ecosystem respiration (Re) in relation to vegetation biomass, species richness, and environmental variables at each point, using an automated chamber system during the 2005 growing season. Mean light-saturated NEP and GPP were 30.3 and 40.5 μmol CO<sub>2</sub> m<sup>-2</sup> s<sup>-1</sup> [coefficient of variation (CV), 42.7 and 29.4], respectively. Mean Re at 20°C soil temperature, Re<sub>20</sub>, was −10.9 μmol CO<sub>2</sub> m<sup>-2</sup> s<sup>-1</sup> (CV, 27.3). Re<sub>20</sub> was positively correlated with vegetation biomass. GPP<sub>max</sub> was positively correlated with species

richness, but 2 of the 14 points were outliers. Vegetation biomass was the main determinant of spatial variation of Re, whereas species richness mainly affected that of GPP, probably reflecting the complexity of canopy structure and light partitioning in this small grassland patch.

**Keywords** Ecosystem CO<sub>2</sub> flux · Ecosystem structure and functioning · Spatial heterogeneity · Species richness · Qinghai-Tibetan plateau

### Introduction

Grassland ecosystems, which cover 24% of the terrestrial surface (Sims and Risser 2000) and have a high capacity to act as a carbon sink (Scurlock and Hall 1998; Scurlock et al. 2002), play an important role in the global carbon cycle. Recent reports on the possible influence of global climate change on terrestrial ecosystems predict a remarkable impact on vegetation growing at high altitudes and high latitudes (Høye et al. 2007; IPCC 2007), including structural and functional changes caused by the extinction or limited growth of species (Chapin 2003; Van der Wal 2006). Therefore, it is of critical importance to reveal the how grassland structure and distribution affect carbon sequestration. However, the sink strength of the world's grasslands has yet to be well quantified, mainly because of the large temporal and spatial variations in the CO<sub>2</sub> flux of grassland ecosystems (e.g., Kim et al. 1992; Flanagan et al. 2002; Xu and Baldocchi 2004). The ecosystem CO<sub>2</sub> flux can vary spatially at both large scales, such as at the level of climate zones, and small scales, such as at the micro-habitat level (Kicklighter et al. 1999; Gilmanov et al. 2007; Risch and Frank 2006). Characterizing the large-scale

M. Hirota (✉) · P. Zhang  
Graduate School of Life and Environmental Sciences,  
University of Tsukuba, 1-1-1 Tennodai, Tsukuba,  
Ibaraki 305-8572, Japan  
e-mail: hirota@biol.tsukuba.ac.jp; hirota0313@gmail.com

S. Gu · Y. Li  
Northwest Plateau Institute of Biology,  
Chinese Academy of Sciences, Xining 810001,  
People's Republic of China

H. Shen · Y. Tang  
National Institute for Environmental Studies,  
Onogawa 16-2, Tsukuba, Ibaraki 305-8506, Japan

T. Kuriyama  
Department of Biology, Faculty of Science,  
Toho University, 2-2-1 Miyama, Funabashi,  
Chiba 274-8510, Japan

spatial CO<sub>2</sub> flux variation (Turner et al. 2003; Kato and Tang 2008) is necessary for precise estimation of the CO<sub>2</sub> sink strength of the world's extensive and diverse grasslands. Understanding the small-scale spatial variation of the CO<sub>2</sub> flux is also very important, for two main reasons. First, the CO<sub>2</sub> flux is strongly dependent on the distribution and species composition of the vegetation, which show a high degree of small-scale spatial variability (Bubier et al. 2006), mainly because each species has species-specific ecophysiological traits. Second, the distribution and species composition of vegetation may be easily altered by environmental change (Chapin 2003); therefore, CO<sub>2</sub> flux is likely to show small-scale variability reflecting vegetation changes caused by environmental change.

Small-scale spatial variation of ecosystem CO<sub>2</sub> flux (i.e., at the meter to centimeter level) can be caused by various abiotic and biotic factors and their interactions (Risch and Frank 2006; Sjögersten et al. 2006; Shaver et al. 2007; Street et al. 2007). Previous studies have shown that abiotic factors such as hydrological variation and soil carbon content may control small-spatial-scale variation in both gross primary production (GPP) and ecosystem respiration (Re) in grasslands (Sjögersten et al. 2006; Risch and Frank 2006). Furthermore, biotic factors such as grazing intensity (Wilsey et al. 2002), vegetation biomass (Risch and Frank 2006; Hirota et al. 2009; Zhang et al. 2009), leaf area index (LAI; Shaver et al. 2007; Street et al. 2007), and leaf nitrogen content (Risch and Frank 2006; Arndal et al. 2009) are also recognized as being among the main factors controlling small-scale spatial variations in GPP and net ecosystem production (NEP) in grasslands. In contrast, little information is available on the relationship between species richness and small-scale spatial variation of the ecosystem CO<sub>2</sub> flux, though species richness has been demonstrated to be a major determinant of above-ground biomass and net primary productivity in grasslands (e.g., Loreau and Hector 2001; Tilman et al. 2001). Given the strong relationship between species richness and productivity, species richness should also affect small-scale spatial CO<sub>2</sub> flux variation in grassland ecosystems. Thus, we aimed to reveal the possible effects of species richness and vegetation biomass on CO<sub>2</sub> flux in a high-altitude grassland characterized by high spatial heterogeneity in the distribution of vegetation in terms of species composition and biomass.

Alpine meadows such as *Kobresia* meadows on the Qinghai-Tibetan plateau are potentially suitable ecosystems for investigating spatial CO<sub>2</sub> flux heterogeneity because direct CO<sub>2</sub> flux measurement is relatively easy owing to the small size of the plants. For example, Chen et al. (2007) recently reported high plant species richness at very small scales (16–20 species per 0.01 m<sup>2</sup>) in an alpine meadow on the plateau. It is also noteworthy that

the *Kobresia* meadows on the plateau are very likely to be a huge sink for atmospheric CO<sub>2</sub>, and several studies have assessed CO<sub>2</sub> exchange at a large spatial scale using the eddy-covariance system (Kato et al. 2004; Gu et al. 2005; Zhao et al. 2006). In contrast, little is known about how ecosystem CO<sub>2</sub> flux may vary at small-spatial scales or about the environmental factors that determine its spatial variation. Moreover, because alpine ecosystems are predicted to be extremely sensitive to environmental changes such as global warming (e.g., Diaz et al. 2003), high-resolution estimates of ecosystem CO<sub>2</sub> flux and its relationship with vegetation properties, which are likely to be affected by such environmental changes, are valuable for predicting the consequences of such changes. In this study, we considered the instantaneous ecosystem CO<sub>2</sub> flux components NEP, Re, and GPP, obtained using the closed-chamber method (Hirota et al. 2006, 2009; Zhang et al. 2009), to be characteristics of CO<sub>2</sub> sink strength, and we investigated the small-spatial-scale variation in these parameters in relation to that in vegetation properties. This measurement technique can be used for accurate small-scale observations of both ecosystem CO<sub>2</sub> flux and related vegetation properties, whereas the eddy-covariance technique is more suitable for larger scale observations.

Our major objectives were (1) to characterize the magnitudes of three ecosystem CO<sub>2</sub> fluxes, NEP, daytime Re, and GPP, in relation to species richness, species composition, and vegetation biomass, and (2) to clarify the underlying mechanisms regulating small-scale spatial variation in these fluxes in a *Kobresia* meadow.

## Study site and methods

### Study site

Ecosystem CO<sub>2</sub> flux measurements were conducted in an alpine meadow on the Qinghai-Tibetan plateau. The study site is at the northern edge of the plateau (37°36'47"N, 101°18'24"E; 3,250 m a.s.l.). Topographically, the meadow is fairly flat, and it is situated in a wide intermountain grassland basin. From 1981 to 2000, the annual mean air temperature was -1.7°C and the annual precipitation was 561 mm. The soil is a clay loam, and its average thickness is 65 cm. The top 5–10 cm of the soil is wet and high in organic matter. Details are given elsewhere (Kato et al. 2004; Gu et al. 2005). This alpine meadow is dominated by three perennial sedges, *Kobresia humilis* (C.A.Mey. ex Trautv.) Serg., *Kobresia pygmaea* C.B.Clarke ex Hook.f., and *Kobresia tibetica* Maxim. (Li and Zhou 1998). The growing period is May to October. From 1980 to 1993, the maximum above-ground biomass varied within the range

of  $342 \pm 50$  g dry weight (DW)  $m^{-2}$  (average  $\pm$  SD) during summer, and LAI peaked at about 4 in July (Li and Zhou 1998). The study site is grazed by yaks and sheep every winter.

#### Sampling design

To examine the spatial variation in the  $\text{CO}_2$  flux and the relationship between the flux and the vegetation composition within the alpine meadow, we chose a flat area ( $30 \text{ m} \times 40 \text{ m}$ ) about 300 m east of a micrometeorological flux tower (Fig. 1) for intensive study. On 8 July 2005, more than a week before our flux measurements began, we randomly chose 14 points by throwing 14 small markers into the intensive study area, with our eyes closed so that distances between the points would not be equal. The minimum distance was 0.5 m, and the maximum was 30 m. Then, we installed a stainless-steel base at soil level (30 cm in diameter  $\times$  20 cm high) at each point to reduce the influence of vegetation and soil disturbances on the ecosystem  $\text{CO}_2$  flux measurements. At the 14 points, we measured the net ecosystem  $\text{CO}_2$  exchange (NEE) under different light conditions, as well as the soil temperature and soil moisture, between 0900 hours and 1600 hours (Beijing Standard Time) from 15 to 30 July. On 31 July, after the final flux measurement, we sampled and quantified the vegetation biomass at each point.

#### Net ecosystem $\text{CO}_2$ exchange

The custom-made, multi-channel, automated chamber system consisted of four transparent acrylic chambers (30 cm in diameter  $\times$  30 cm high, with a wall thickness of 3 mm) and a control box (Fig. 1). Each chamber had a removable lid. Silicone tape was used to seal the joint between the lid and the chamber wall. The lid was gently opened and closed by a double-acting pneumatic cylinder (RCC2 series, CKD, Aichi, Japan). The air supply for the pneumatic cylinder was provided by a small air compressor (3IMP-0.5, JUN-AIR International, Nørresundby, Denmark), and a portable personal computer was used to control the timing of the opening and closing of the lid. We set the period of closure to 150 s for measurement of ecosystem  $\text{CO}_2$  fluxes. Measured variables were the concentration of atmospheric  $\text{CO}_2$  in the chamber, photosynthetically active radiation (PAR), relative humidity (RH), air temperature inside and outside the chamber, soil temperature at a 5-cm depth, and the pressure differential between the inside and outside of the chamber.  $\text{CO}_2$  was directly monitored by a  $\text{CO}_2$  probe, which was a silicon-based non-dispersive infrared sensor (GMP343, Vaisala, Helsinki, Finland). PAR was measured with a quantum sensor (IKS-27, Koito Industries, Kanagawa, Japan), and

RH and air temperature were measured with a temperature/RH probe (HMP50, Vaisala). The pressure differential was recorded with a pressure sensor (NPH-8, GE Sensing Japan, Tokyo, Japan; Fig. 1). All data were recorded by a data logger (8422-50, Hioki, Nagano, Japan) at intervals of 1 s. To control the air temperature inside the chamber while it was closed, we used an electronic cooler (FTA951, Ferrotec, Tokyo, Japan) controlled by a proportional-integral-derivative (PID) controller (TTM1520, Toho Electronics, Tokyo, Japan). Two small DC-powered fans mixed the air inside the chamber. With this cooling system, we could maintain the air temperature within the chamber while it was closed at no more than  $1.2^\circ\text{C}$  above the outside air temperature. The pressure differential between the inside and outside scarcely changed during opening and closing of the chamber, because the slow movement of the lid barely disturbed the air system inside the chamber. Minimization of pressure changes within the chamber is critical for flux measurements (Lund et al. 1999; Davidson et al. 2002).

We calculated NEE ( $\mu\text{mol CO}_2 \text{ m}^{-2} \text{ s}^{-1}$ ) from the temporal change in  $\text{CO}_2$  concentration during the closure period as:

$$\text{NEE} = \frac{d\text{CO}_2/dt}{dt} \times P/[R(273.15 + T)]V/A, \quad (1)$$

where  $d\text{CO}_2/dt$  is the slope of the change in  $\text{CO}_2$  concentration in the chamber in relation to time ( $\mu\text{mol mol}^{-1} \text{ s}^{-1}$ );  $P$  is atmospheric pressure (kPa);  $R$  is the gas constant, 8.314 (kPa  $\text{m}^3 \text{ K}^{-1} \text{ mol}^{-1}$ );  $T$  is the air temperature inside the chamber ( $^\circ\text{C}$ );  $V$  is the chamber volume ( $\text{m}^3$ ); and  $A$  is the chamber bottom area ( $\text{m}^2$ ). To obtain a linear relationship between  $\text{CO}_2$  concentration and time in the shortest possible time, we used only data collected from 30 s to 90 s after chamber closure. To measure the daytime RE and to obtain light-response curves, we measured NEE under 65% light, using a shade screen over the chamber, and 0% light, using a completely dark cloth, right after the NEE measurement under 100% light. It took about 10 min to perform the NEE measurements under the three light conditions at each point. To quantify the NEE at the 14 points as close to simultaneously as possible, we measured NEE at four points and then relocated all the chambers to another four points. It took about 1 min to set the four chambers up at the next four points. Because there were 14 points, the final series of measurements was performed at only two points. To minimize the impact on the measurement data of setting up the chambers, we waited at least 1 min after setting up the chamber before measuring the  $\text{CO}_2$  flux. In total, one measurement cycle at all 14 points required about 50 min. Hence, NEE was measured at each point about every 50 min between 0900 hours and 1600 hours, i.e., seven or eight times per day. So that we could compare NEE among the 14 points under weather

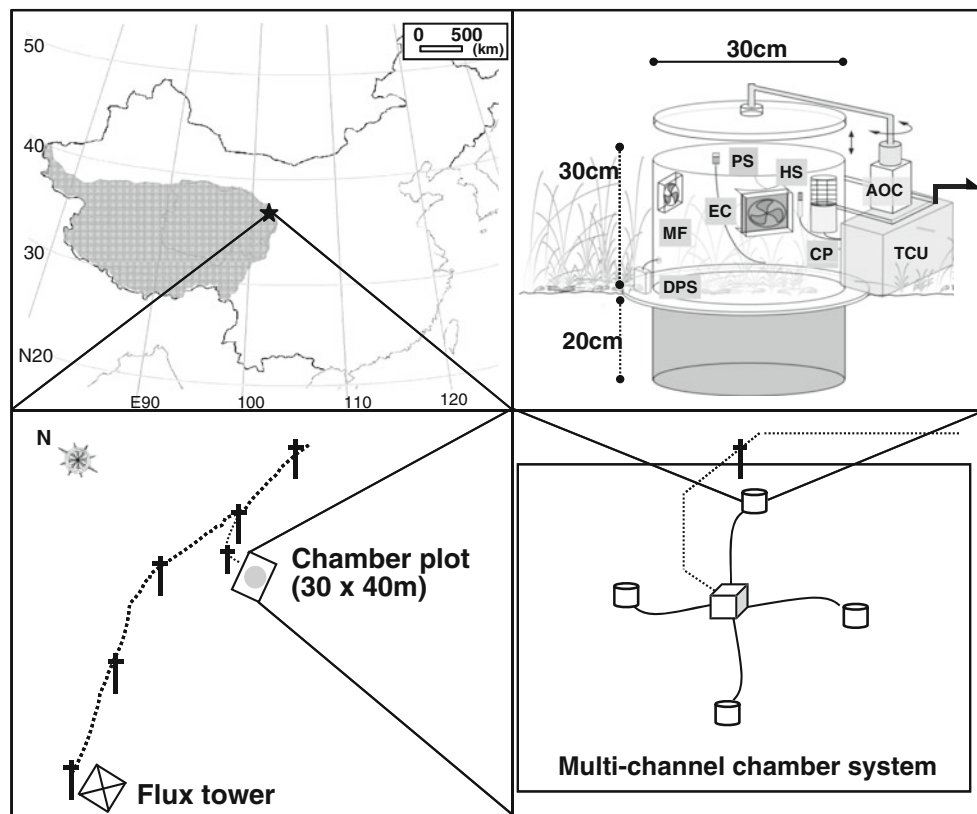


**Fig. 1** Location of the study site and layout of the ecosystem flux measurement site, showing the location of the micrometeorological tower and the chamber measurement plot (30 m × 40 m; *lower left figure*). Tall crosses and dotted line in the *lower left figure* represent utility poles and electricity wires. The distance between the tower and the study area was about 300 m. In the *lower right figure*, the four cylinders and the box represent the net ecosystem CO<sub>2</sub> exchange

conditions that were as similar as possible, we used only those data obtained under clear-sky conditions between 15 and 30 July 2005. We defined clear sky conditions as no rain or hail, regardless of cloud cover. We also excluded data obtained within 1 h after the cessation of rain or hail. The excluded data accounted for 26.7% of the total data. Air temperature and soil temperature at a 5-cm depth during the daytime measurement period ranged from 15.4 to 27.2°C and from 18.1 to 26.3°C, respectively.

Immediately after the flux measurements, we measured the soil moisture content (v/v) within each measurement point at 0–12 cm soil depth with a soil moisture probe (CD620, Campbell Scientific, Logan, UT).

#### Data analysis

We calculated NEP as –NEE under full light conditions with the chamber uncovered, and adopted a sign convention according to which ecosystem CO<sub>2</sub> uptake is positive and CO<sub>2</sub> emission via respiration is negative. Thornley and Johnson (1990) used a curve-fitting technique to describe

(NEE) chambers and the main system, respectively. The *upper right figure* represents a custom-made automated chamber. *AOC* Automated open/close system; *CP* CO<sub>2</sub> probe, *EC* electronic cooler with micro-fan, *HS* humidity sensor, *PS* photosynthetically active radiation (PAR) sensor, *MF* micro-fan, *DPS* sensor for detecting pressure differential between inside and outside of chamber, *TCU* temperature control unit

the relationship between NEP and PAR based on a rectangular hyperbola:

$$\text{NEP} = (\alpha \text{NEP} \times \text{NEP}_{\max} \times \text{PAR}) / (\alpha \text{NEP} \times \text{PAR} + \text{NEP}_{\max}) + R_{\text{int}}, \quad (2)$$

where  $\alpha \text{NEP}$  is the initial slope of the rectangular hyperbola, also called the “apparent quantum yield,”  $\text{NEP}_{\max}$  is the asymptotic approach to maximum NEP at high light intensity, and  $R_{\text{int}}$  is the y axis intercept, or apparent dark respiration. The observed Re was then regressed exponentially against soil temperature at a 5-cm depth (ST<sub>5</sub>):

$$\text{daytime Re} = a \times \exp(ST_5 \times b), \quad (3)$$

where  $a$  and  $b$  are regression coefficients. The  $Q_{10}$  value, i.e., the rate of change in Re with a change of 10°C in soil temperature (Raich and Schlesinger 1992), is expressed as:

$$Q_{10} = \exp(10 \times b), \quad (4)$$

GPP was calculated from Re and the immediately preceding NEP under full light as:

$$GPP = NEP - Re, \quad (5)$$

The relationship between GPP and PAR is also described by a rectangular hyperbola:

$$GPP = (\alpha GPP \times GPP_{max} \times PAR) / (\alpha GPP \times PAR + GPP_{max}), \quad (6)$$

where  $\alpha GPP$  is the initial slope of the rectangular hyperbola, also called the “apparent quantum yield of GPP,” and  $GPP_{max}$  is the asymptotic approach to maximum GPP at high light intensity. We determined each parameter in Eqs. 2, 3, and 6 at each measurement point using nonlinear regression, minimizing the root-mean-square error by the Gauss–Newton method, with the Systat v. 11 software (Systat Software, Chicago, IL).

To examine the spatial variation in ecosystem  $\text{CO}_2$  flux among the 14 points, we calculated three characteristic parameters ( $GPP_{max}$ ,  $NEP_{max}$ , and  $Re_{20}$ )—the value of daytime  $Re$  at a soil temperature of 20°C. We used a soil temperature of 20°C because that is the approximate mean daytime soil temperature during the growing season in this alpine meadow. We also calculated  $\alpha GPP$ , which is highly relevant to the photosynthesis light-response curve, and  $Q_{10}$ , which is an indicator of the sensitivity to temperature of  $Re$ . We compared the three calculated ecosystem  $\text{CO}_2$  fluxes ( $GPP_{max}$ ,  $NEP_{max}$ , and  $Re_{20}$ ) and the two parameters ( $\alpha GPP$  and  $Q_{10}$ ) among the 14 points, and determined the coefficient of variation (CV) of each to characterize the magnitude of spatial variation of each variable.

#### Vegetation properties

On 31 July we harvested the above-ground biomass (AGB) and the below-ground biomass (BGB) down to a 20-cm soil depth at all measurement points. The AGB was divided by species, dried at 80°C for 2 days, and weighed. BGB was divided into shallow (0–10 cm soil depth, sBGB) and deep (10–20 cm soil depth, dBGB) parts, washed gently in running water, dried at 80°C, and weighed. We defined the species richness at a point as the total number of species within the 30-cm-diameter point.

#### Statistical analyses

Pearson’s correlation coefficient ( $r$ ) and multiple linear regression analysis were used to identify significant associations between ecosystem  $\text{CO}_2$  fluxes and vegetation properties. All data from the 14 points were analyzed by one-way ANOVA, and then differences among means were analyzed with Tukey–Kramer multiple-comparison tests, with the level of statistical significance taken as  $P < 0.01$ . We performed all statistical analyses with the SYSTAT ver. 11 software (Systat Software).

## Results

### Ecosystem $\text{CO}_2$ exchange

Ecosystem  $\text{CO}_2$  flux varied markedly among the 14 points. PAR-saturated  $NEP$  ( $NEP_{max}$ ) differed by 3.9-fold (16.8–64.9  $\mu\text{mol CO}_2 \text{ m}^{-2} \text{ s}^{-1}$ ), PAR-saturated GPP ( $GPP_{max}$ ) by 2.8-fold (24.7–69.3  $\mu\text{mol CO}_2 \text{ m}^{-2} \text{ s}^{-1}$ ), and ecosystem respiration at 20°C and a 5-cm soil depth ( $Re_{20}$ ) by 2.5-fold (−7.5 to −18.9  $\mu\text{mol CO}_2 \text{ m}^{-2} \text{ s}^{-1}$ ; Fig. 2). Mean  $NEP_{max}$  was 30.3  $\mu\text{mol CO}_2 \text{ m}^{-2} \text{ s}^{-1}$  (CV = 42.7), mean  $GPP_{max}$  was 40.5  $\mu\text{mol CO}_2 \text{ m}^{-2} \text{ s}^{-1}$  (CV = 29.4), and mean  $Re_{20}$  was −10.9  $\mu\text{mol CO}_2 \text{ m}^{-2} \text{ s}^{-1}$  (CV = 27.3; Table 1). The apparent quantum yield of GPP ( $\alpha GPP$ ) also varied among the 14 points by 7.4-fold (0.011–0.081 mol  $\text{CO}_2 \text{ mol}^{-1}$  photons), and its mean value was 0.034 mol  $\text{CO}_2 \text{ mol}^{-1}$  photons (CV = 17.4; Fig. 2, Table 1). The temperature sensitivity of  $Re$  ( $Q_{10}$ ) also varied among the 14 points by 2.9-fold (1.3–3.8), with a mean of 2.1 (CV = 16.0; Fig. 2, Table 1). The soil temperature varied from around 18–26°C with time (0900–1600 hours), but values obtained at the same time showed no significant spatial variation among the 14 points ( $P > 0.05$ , mean SD = 1.8,  $n = 14$ ). The soil moisture content also varied temporally from around 35–50% (v/v) and was affected by rain and hail, but values obtained at the same time showed no significant spatial variation among the 14 points ( $P > 0.05$ , mean SD = 2.4,  $n = 14$ ).

### Vegetation properties

Vegetation differed quantitatively and qualitatively among the 14 points (Table 2). AGB of vascular plants differed by 4.0-fold, from 76.2 to 306.7 g DW  $\text{m}^{-2}$ ; sBGB at 0–10 cm soil depth by 6.4-fold, from 427.5 to 2,722.9 g DW  $\text{m}^{-2}$ ; and dBGB at 10–20 cm soil depth by 3.7-fold, from 188.0 to 701.5 g DW  $\text{m}^{-2}$ . The mean values were 155.1, 1,188.7, and 338.6 g DW  $\text{m}^{-2}$ , respectively (Table 1). We identified 55 species belonging to 18 families at the 14 points. Most points were dominated by grasses (Table 2), such as *Festuca ovina* L., *Stipa aliena* Keng., *Elymus nutans* Griseb., and *Poa alpigena* Lindm., *Anaphalis lactea* Maxim., *Aster flaccidus* Bunge., *Oxytropis kansensis* Bunge., *Saussurea nigrescens* Maxim., and *Scirpus distigmaticus* (Kük.) Tang & F.T.Wang were abundant. Species richness varied from 17 to 31 species among the points (mean value = 25.1, Table 1). Judging from the CV values of the vegetation properties, the spatial variation in plant diversity was small compared with that of biomass (Table 1). The species composition of the vegetation at points B and K was unusual compared with the other points: the proportions of the dominant Poaceae and Cyperaceae biomass were very large (78.5% at B and

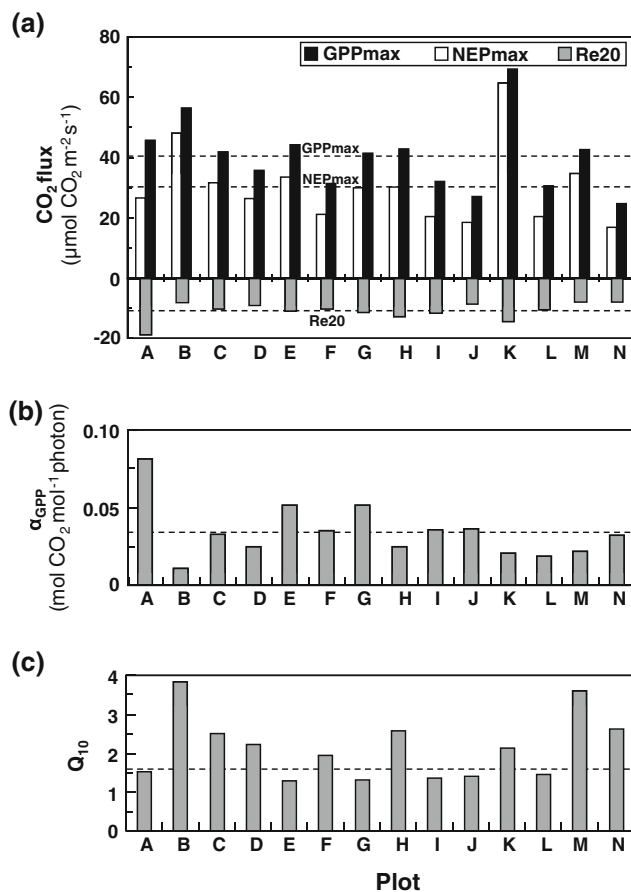


**Fig. 2** **a** Spatial variation in ecosystem CO<sub>2</sub> flux in the 14 measurement points. *Broken lines* means of maximum gross primary production (GPP<sub>max</sub>), net ecosystem production (NEP<sub>max</sub>), and ecosystem respiration (Re<sub>20</sub>). Bars are sorted from high to low above-ground biomass (AGB). **b** Spatial variation in apparent quantum yield of GPP ( $\alpha$ GPP). **c** Spatial variation in temperature sensitivity of Re ( $Q_{10}$ ). *Broken lines* mean values of  $\alpha$ GPP and  $Q_{10}$

72% at K), and species richness was relatively low (23 at B and 17 at K; Table 2).

Vegetation biomass did not correlate significantly with species richness ( $r^2 = 0.11$ ,  $P > 0.001$  for AGB;  $r^2 = 0.15$ ,  $P > 0.001$  for sBGB; and  $r^2 = 0.13$ ,  $P > 0.001$  for dBGB).

#### Relationship between ecosystem CO<sub>2</sub> flux and vegetation properties

Regression analyses using all 14 sets of data showed that NEP<sub>max</sub> and GPP<sub>max</sub> were not significantly correlated with any biomass component or with species richness (Table 3). More than 60% of the variation in Re<sub>20</sub> among the points, however, could be explained by vegetation biomass [sBGB,  $r^2 = 0.66$ ,  $P < 0.001$ ; total biomass (TB),  $r^2 = 0.62$ ,  $P < 0.001$ ]. Apparent quantum yield for GPP ( $\alpha$ GPP) was positively correlated with both AGB and

**Table 1** Mean values and coefficients of variation (CV, %) of ecosystem CO<sub>2</sub> flux, its response to light intensity ( $\alpha$ ) for gross primary production (GPP) and temperature for ecosystem respiration (Re;  $Q_{10}$ ), and vegetation properties

	Mean value	CV (%)
Net CO <sub>2</sub> flux		
Re <sub>20</sub> (μmol CO <sub>2</sub> m <sup>-2</sup> s <sup>-1</sup> )	-10.9	27.3
GPP <sub>max</sub> (μmol CO <sub>2</sub> m <sup>-2</sup> s <sup>-1</sup> )	40.5	29.4
NEP <sub>max</sub> (μmol CO <sub>2</sub> m <sup>-2</sup> s <sup>-1</sup> )	30.3	42.7
Response characteristics of CO <sub>2</sub> flux		
$\alpha$ GPP (mol CO <sub>2</sub> mol <sup>-1</sup> photons <sup>-1</sup> )	0.034	17.4
$Q_{10}$	2.1	16
Vegetation properties		
AGB (g DW m <sup>-2</sup> )	155.1	36.2
sBGB (g DW m <sup>-2</sup> )	1,188.7	49.8
dBGB (g DW m <sup>-2</sup> )	338.6	37.1
Species richness	25.1	14.6

NEP Net ecosystem production, AGB above ground biomass, BGB below ground biomass

sBGB ( $r^2 = 0.38$ ,  $P = 0.022$ , and  $r^2 = 0.32$ ,  $P = 0.046$ , respectively; Table 3). The temperature sensitivity of Re,  $Q_{10}$ , was not significantly correlated with any variable.

Further regression analyses with 12 sets of data (excluding the data from points B and K, which had relatively simple species compositions dominated by the Poaceae and Cyperaceae) gave different results. NEP<sub>max</sub> and GPP<sub>max</sub> showed significant positive correlations with species richness ( $r^2 = 0.53$ ,  $P < 0.001$ , and  $r^2 = 0.66$ ,  $P < 0.001$ , respectively; Fig. 3), and more than 72% of the variation in  $\alpha$ GPP could be explained by biomass (AGB,  $r^2 = 0.79$ ,  $P < 0.01$ ; sBGB,  $r^2 = 0.62$ ,  $P = 0.044$ ; TB,  $r^2 = 0.72$ ,  $P < 0.001$ ). Re<sub>20</sub> was similarly positively correlated with biomass components (AGB,  $r^2 = 0.35$ ,  $P = 0.042$ ; sBGB,  $r^2 = 0.66$ ,  $P < 0.001$ ; TB,  $r^2 = 0.62$ ,  $P < 0.001$ , Table 3).

#### Discussion

##### Characteristics of spatial variation of ecosystem CO<sub>2</sub> flux in an alpine meadow

In this study, to examine the range of spatial variation of ecosystem CO<sub>2</sub> flux under similar conditions, we calculated three characteristic parameters, NEP<sub>max</sub>, GPP<sub>max</sub>, and Re<sub>20</sub>, and two additional variables,  $\alpha$ GPP and  $Q_{10}$ , which are related strongly to the light-response curve of GPP and to the sensitivity to temperature of Re, respectively, as parameters suitable for comparison, at least during the study period. These five parameters showed large spatial variation within an area of about 1,200 m<sup>2</sup> (Fig. 2). Within

**Table 2** Biomass ( $\text{g DW m}^{-2}$ ), number of vascular plant species, and list of dominant vascular plant species in each measurement point. AGB and BGB were recorded on 29 July 2005 following flux measurement

Point	AGB ( $\text{g DW m}^{-2}$ )	sBGB ( $\text{g DW m}^{-2}$ )	dBGB ( $\text{g DW m}^{-2}$ )	Species richness	Vegetation composition (relative biomass, %)
A	306.7	2,722.9	408.4	26	Poaceae (48.0), <i>Aster flaccidus</i> Bunge (9.7), <i>Morina chinensis</i> (Batal. ex Diels) Pai (9.5)
B	204.1	1,298.2	285.9	23	Poaceae (75.8), <i>Kobresia humilis</i> <sup>a</sup> (C.A.Mey. ex Trautv.) Serg. (2.4), <i>Aster flaccidus</i> Bunge (2.4)
C	187.7	1,405.0	314.8	28	Poaceae (45.3), <i>Saussurea nigrescens</i> Maxim. (12.4), <i>Kobresia humilis</i> <sup>a</sup> (C.A.Mey. ex Trautv.) Serg. (10.7)
D	173.7	839.1	355.8	25	<i>Anaphalis lactea</i> Maxim. (19.2), Poaceae (17.7), <i>Aster flaccidus</i> Bunge (12.3)
E	171.1	1,234.7	246.3	31	Poaceae (46.2), <i>Oxytropis kansuensis</i> Bunge (13.2), <i>Gentiana farreri</i> Balf.f. (5.4)
F	170.3	1,228.0	404.1	27	Poaceae (29.6), <i>Lancea tibetica</i> Hook.f. & Thomson (14.1), <i>Gentiana farreri</i> Balf.f. (9.1)
G	158.0	1,212.6	201.3	26	<i>Scirpus distigmaticus</i> <sup>a</sup> (Kük.) Tang & F.T.Wang (20.5), Poaceae (16.0), <i>Saussurea nigrescens</i> Maxim. (17.9)
H	132.8	846.0	188.0	28	Poaceae (35.5), <i>Scirpus distigmaticus</i> <sup>a</sup> (Kük.) Tang & F.T.Wang (10.1), <i>Saussurea nigrescens</i> Maxim. (10.8)
I	126.1	829.6	259.3	25	Poaceae (35.5), <i>Saussurea nigrescens</i> Maxim. (10.8), <i>Scirpus distigmaticus</i> <sup>a</sup> (Kük.) Tang & F.T.Wang (10.1)
J	122.7	1,058.7	315.9	23	<i>Anaphalis lactea</i> Maxim. (18.9), Poaceae (17.5), <i>Leontopodium nanum</i> Hand.-Mazz. (11.8)
K	117.5	2,063.3	701.5	17	Poaceae (41.9), <i>Kobresia humilis</i> <sup>a</sup> (C.A.Mey. ex Trautv.) Serg. (17.8), <i>Scirpus distigmaticus</i> <sup>a</sup> (Kük.) Tang & F.T.Wang (11.3)
L	112.7	664.8	356.0	27	Poaceae (32.0), <i>Aster flaccidus</i> Bunge (20.0), <i>Medicago ruthenica</i> Trautv. (11.2)
M	112.1	811.2	313.0	27	<i>Saussurea nigrescens</i> Maxim. (26.8), Poaceae (24.2), <i>Scirpus distigmaticus</i> <sup>a</sup> (Kük.) Tang & F.T.Wang (16.4)
N	76.2	427.5	389.7	19	<i>Aster flaccidus</i> Bunge (24.9), <i>Saussurea nigrescens</i> Maxim. (21.2), <i>Lancea tibetica</i> Hook.f. & Thomson (14.7)

Points were named A–N in order of size of AGB for convenience. Vegetation in points B and K had large contributions from Poaceae and Cyperaceae biomass (78.5% in B and 72% in K)

<sup>a</sup> Species belonging to Cyperaceae

**Table 3** Pearson's coefficient of correlation ( $r$ ) among vegetation properties, three ecosystem CO<sub>2</sub> fluxes, and two parameters,  $\alpha$ GPP and  $Q_{10}$ , using all data ( $n = 14$ )

Vegetation properties	Ecosystem CO <sub>2</sub> flux			Parameters of GPP and Re	
	NEP <sub>max</sub>	Re <sub>20</sub>	GPP <sub>max</sub>	$\alpha$ GPP	$Q_{10}$
AGB	-0.09	0.59*	-0.29	-0.62*	-0.85
sBGB	-0.49	0.81***	-0.43	-0.57*	-0.18
dBGB	-0.50	0.30	-0.43	0.12	-0.02
TB	-0.50	0.79***	-0.63	-0.52	-0.15
Species richness	0.35	0.03	0.23	-0.29	-0.19
Soil moisture content	0.11	-0.03	0.04	-0.15	-0.13

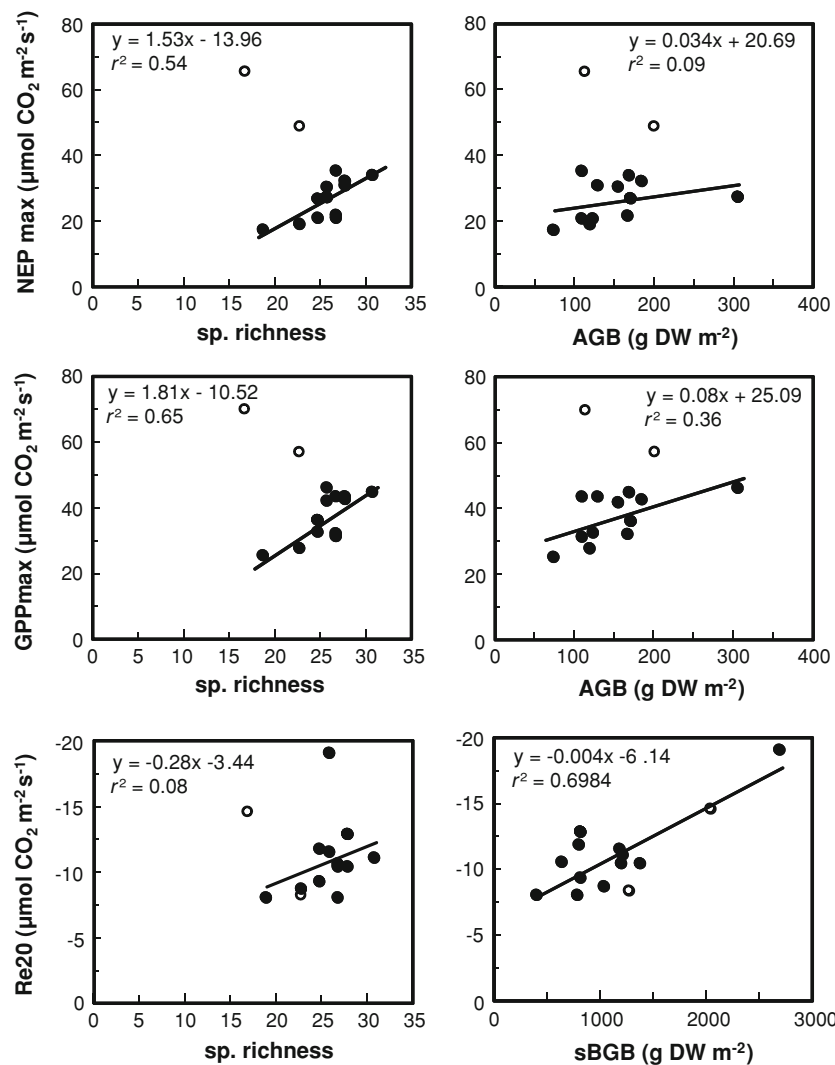
sBGB Shallow below-ground biomass, dBGB deep below-ground biomass, TB total biomass

\*  $P < 0.05$ , \*\*  $P < 0.01$ , \*\*\*  $P < 0.001$

a small, flat area, spatial variations in light availability above the plant canopy, as well as those in air temperature and air humidity, should be very limited. Although soil temperature and soil moisture did not differ significantly

among the points ( $P > 0.05$ ), vegetation biomass, vegetation composition, and species richness were different among the 14 measurement points (Table 2). Furthermore, spatial CVs were similar between the CO<sub>2</sub> flux variables of

**Fig. 3** Relationships between species richness and ecosystem CO<sub>2</sub> fluxes: NEP<sub>max</sub>, GPP<sub>max</sub>, and Re<sub>20</sub> (left); between AGB or shallow below-ground biomass (sBGB) and NEP<sub>max</sub>, GPP<sub>max</sub>, and Re<sub>20</sub> (right). Open symbols Data from points F and I, which contained large contributions from the Poaceae and Cyperaceae in their biomass (see Table 2). The solid line in each graph represents linear regression using only the black symbols ( $n = 12$ ), excluding data from points F and I



NEP<sub>max</sub>, GPP<sub>max</sub>, and Re<sub>20</sub> and biomass. These results suggest that vegetation properties, including plant biomass and species richness, determined the small-scale heterogeneity of these CO<sub>2</sub> fluxes.

Similar results have been reported for arctic ecosystems (Sjögersten et al. 2006; Shaver et al. 2007; Street et al. 2007) and other alpine grasslands (Arndal et al. 2009; Hirota et al. 2009). Risch and Frank (2006) demonstrated that spatio-temporal variations in GPP, Re, and NEP in a temperate grassland were related to differences in AGB and total shoot nitrogen content. Street et al. (2007) found that LAI was the main factor determining the spatial variation of GPP: about 80% of the variation in GPP among sites with various plant species could be explained by the variation in LAI. Uchida et al. (2009) investigated factors controlling NEP in a high-latitude arctic ecosystem during the non-snow period and showed that the coverage and growth of the dominant vascular plant, *Salix polaris* Wahlenb., were the main factors controlling summer NEP.

Hence, such quantitative aspects of vegetation have been considered important factors causing small-scale heterogeneity of ecosystem CO<sub>2</sub> flux. In contrast, the importance of qualitative aspects of vegetation such as species richness to small-scale heterogeneity of ecosystem CO<sub>2</sub> flux has been less well understood. Our results demonstrate that a key factor affecting spatial variation in GPP is species richness, and a key factor affecting that in Re is biomass (Table 3).

#### Vegetation biomass affects ecosystem respiration

Re is the sum of respiration by above- and below-ground plant parts and soil microbes. Thus, our finding of a significant and high correlation between Re and vegetation biomass (Table 3) can probably be attributed to a high contribution of plant respiration to Re and to facilitation of soil microbe respiration by the supply of degradable organic matter from plants (Meharg and Killham 1995;

Farrar et al. 2003). A similar positive correlation between Re and vegetation biomass has been reported for similar, fairly humid grassland ecosystems (Wang et al. 2005; Zhang et al. 2009). However, Nakano et al. (2008) found no such significant correlation in an arid grassland in Inner Mongolia. The strong positive correlation that we found between Re and vegetation biomass, but not between Re and species richness (Table 3, Fig. 3), suggests that the quantity of vegetation, rather than its quality, is the essential factor causing spatial variation in Re.

The sensitivity of Re to soil temperature, described by  $Q_{10}$ , also showed large small-scale heterogeneity (CV = 16, Table 1) in this study, but  $Q_{10}$  was not significantly correlated with vegetation properties or soil moisture (Table 3). Many other studies estimating  $Q_{10}$  based on microbial respiration have reported that a large heterogeneity of  $Q_{10}$  is determined mainly by the quality relevant to decomposability of the soil organic matter (e.g., Canadell et al. 2000; Knorr et al. 2005; Fierer et al. 2006). Therefore, it is likely that the spatial variation of the  $Q_{10}$  in this study was mainly controlled not by vegetation properties or soil moisture but by the quality of the soil organic matter. To examine this possibility, further studies on  $Q_{10}$  calculated from data obtained over a wider temperature range and on the qualitative and quantitative properties of the soil organic matter are required.

#### Species richness affects GPP

Our results demonstrated that  $GPP_{max}$  was positively correlated with species richness rather than with vegetation biomass, except at the two outlier points (Fig. 3). The possible positive relationship that we identified might be attributable to efficient light utilization resulting from the complementary effects of the different architectures in the plant canopy structure or to different photosynthetic light utilization efficiencies of leaves (such as sun and shade leaves) among species, as suggested by Anten and Hirose (1999, 2003) and Vojtech et al. (2008). Further observation and analysis on canopy architecture of different species, however, are needed to confirm the speculation. We found, on the other hand, no significant relationships between the community ABG and species richness in this study. In many grasslands, species richness seems to be the major determinant of AGB or NPP (e.g., Loreau and Hector 2001; Tilman et al. 2001). The lack of correlation between species richness and AGB may partly due to some disturbance such as grazing of livestock. Further experimental approaches are needed to clarify the effect of species richness on community biomass in the alpine ecosystem.

Both outlier points (B and K) had very high Poaceae and Cyperaceae biomass (78.5% in B and 72% in K; Table 2) and high  $GPP_{max}$  and  $NEP_{max}$  (Fig. 3) despite their relatively

low species richness and large biomass. One possible explanation for these findings is that these two groups of species, which are often the dominant species in *Kobresia* alpine meadows (Li and Zhou 1998), may have relatively high photosynthetic capacity and productivity, since dominant species generally have large bodies and are able to preferentially take advantage of limited resources (Grime 2001). To demonstrate the underlying mechanisms of how species richness affects productivity, species-specific eco-physiological performance and complementary effects in plant communities with various species compositions should be examined more carefully.

#### Implications of spatial variation in ecosystem $CO_2$ flux at a small scale in an alpine meadow

A rapidly growing number of studies have estimated terrestrial  $CO_2$  flux at various scales by remote sensing and modeling approaches (e.g., Kicklighter et al. 1999; Turner et al. 2003; Ito 2008). An understanding of the spatial variation in vegetation properties and ecosystem  $CO_2$  flux at the landscape and biome levels is essential if we are to estimate ecosystem carbon budgets with high accuracy. However, we believe that demonstrating these spatial variations and clarifying their underlying mechanisms at small scales are of equal importance, for the following reasons.

First, demonstrating the relationships between ecosystem  $CO_2$  flux and vegetation properties is essential for understanding the relative roles played by biomass and biodiversity at the community level, one of the central challenges in community and ecosystem ecology today (Loreau et al. 2002). Second, demonstrating each major factor influencing the spatial variation in ecosystem production and ecosystem respiration will help us to accurately predict  $CO_2$  sink strength in high-altitude ecosystems under future climate conditions. It is highly likely that environmental change due to global and local disturbances will alter not only the vegetation biomass but also the species composition within an ecosystem. Especially in fragile ecosystems such as the high-altitude ecosystems of our study area, which are easily influenced by environmental change, the vegetation structure will alter drastically under future climate conditions. One recent study has suggested that climate warming will reduce species richness in alpine meadows on the Qinghai-Tibetan plateau (Klein et al. 2004). If species richness decreases, but with little change in vegetation biomass under future warming, ecosystem productivity expressed as GPP in *Kobresia* meadows may decrease, as suggested by the results of this study. Further research focused on the spatial variation of ecosystem  $CO_2$  flux with vegetation properties, including biomass and species composition, at small-scale is therefore needed.

**Acknowledgments** We thank Professor Jingyun Fang and Associate Professor Wei Wang at the Peking University for providing fieldwork support and technical assistance. This study was part of a joint research project between the National Institute for Environmental Studies, Japan, and the Northwest Institute of Plateau Biology, China, as part of the “Integrated Study for Terrestrial Carbon Management of Asia in the 21st Century Based on Scientific Advancements” and “Early Detection and Prediction of Climate Warming Based on the Long-Term Monitoring of Alpine Ecosystems on the Tibetan Plateau” projects. This study was supported by the One Hundred Talent Project (0429091211), by Grants-in-Aid for Scientific Research from the Japan Society for the Promotion of Science (JSPS; No. 18710017), and by the JSPS-KOSEF-NSFC A3 Foresight Program (Quantifying and Predicting Terrestrial Carbon Sinks in East Asia: Toward a Network of Climate Change Research).

## References

- Anten NPR, Hirose T (1999) Interspecific differences in aboveground growth patterns result in spatial and temporal partitioning of light among species in a tall-grass meadow. *J Ecol* 87:583–597
- Anten NPS, Hirose T (2003) Shoot structure, leaf physiology, and daily carbon gain of plant species in a tallgrass meadow. *Ecology* 84:955–968
- Arndal MF, Illeris L, Michelsen A, Albert K, Tamstorf M, Hansen BU (2009) Seasonal variation in gross ecosystem production, plant biomass, and carbon and nitrogen pools in five high arctic vegetation types. *Arct Antarct Alp Res* 41:164–173
- Bubier JL, Moore TR, Crosby G (2006) Fine-scale vegetation distribution in a cool temperate peatland. *Can J Bot* 84:910–923
- Canadell JG, Mooney HA, Baldocchi DD, Berry JA, Ehleringer JR, Field CB, Gower ST, Hollinger DY, Hunt JE, Jackson RB, Running SW, Shaver GR, Steffen W, Trumbore SE, Valentini R, Bond BY (2000) Carbon metabolism of the terrestrial biosphere: a multitechnique approach for improved understanding. *Ecosystems* 3:115–130
- Chapin FS III (2003) Effects of plants traits on ecosystem and regional processes: a conceptual framework for predicting the consequences of global change. *Ann Bot* 91:455–465
- Chen J, Yamamura Y, Hori Y, Shiyomi M, Yasuda T, Zhou H, Li Y, Tang Y (2007) Small-scale species richness and its spatial variation in an alpine meadow on the Qinghai-Tibet Plateau. *Ecol Res* 23:657–663
- Davidson EA, Savage K, Verchot LV, Navarro R (2002) Minimizing artifacts and biases in chamber-based measurements of soil respiration. *Agric For Meteorol* 113:21–37
- Diaz HF, Eischeid JK, Duncan C, Bradley RS (2003) Variability of freezing levels, melting season indicators, and snow cover for selected high-elevation and continental regions in the last 50 years. *Clim Change* 59:33–52
- Farrar J, Hawes M, Jones D, Lindow S (2003) How roots control the flux of carbon to the rhizosphere. *Ecology* 84:827–837
- Fierer N, Colman B, Schimel JP, Jackson PB (2006) Predicting the temperature dependence of microbial respiration in soil: a continental-scale analysis. *Glob Biogeochem Cycles* 20:GB3026. doi:10.1029/2005GB002644
- Flanagan LB, Wever LA, Carlson PJ (2002) Seasonal and interannual variation in carbon dioxide exchange and carbon balance in a northern temperate grassland. *Glob Change Biol* 8:599–615
- Gilmanov TG, Soussana JF, Allards AL, Ammann C, Balzalero M, Barza Z, Bernhofer C, Campbell CL, Cescatti A, Clifton-Brown J, Dirks BOM, Dore S, Eugster W, Fuhrer J, Gimeno C, Gruenwald C, Haszpra L, Hensen A, Ibrom A, Jacobs AFG, Jones MB, Laurila G, Lohila A, Manca G, Marcolla B, Nagy Z, Pilegaard K, Pinter K, Pio C, Raschi A, Rogiers N, Sanz MJ, Stefani P, Sutton M, Tuba Z, Valentini R, Williams ML, Wohlfahrt G (2007) Partitioning European grassland net ecosystem CO<sub>2</sub> exchange into gross primary productivity and ecosystem respiration using light response function analysis. *Agric Ecosyst Environ* 121:93–120
- Grime JP (2001) *Plant strategies, vegetation processes, and ecosystem properties*, 2nd edn. Wiley, London
- Gu S, Tang Y, Cui X, Kato T, Du M, Li Y, Zhao X (2005) Energy exchange between the atmosphere and a meadow ecosystem on the Qinghai-Tibetan Plateau. *Agric For Meteorol* 129:175–185
- Hirota M, Tang Y, Hu Q, Hirata S, Kato T, Mo W, Cao G, Mariko S (2006) Carbon dynamics in a deep-water wetland on the Qinghai-Tibetan Plateau. *Ecosystems* 9:673–688
- Hirota M, Zhang P, Gu S, Du M, Shimono A, Shen H, Li Y, Tang Y (2009) Altitudinal variation of ecosystem CO<sub>2</sub> fluxes in an alpine grassland from 3600 to 4200 m. *J Plant Ecol* 2:197–205
- Høye TT, Post E, Meltofte H, Schmidt NM, Forchhammer MC (2007) Rapid advancement of spring in the High Arctic. *Curr Biol* 17:R449–R451
- IPCC (2007) *Climate change 2007: the physical science basis*. Cambridge University Press, Cambridge
- Ito A (2008) The regional carbon budget of East Asia simulated with a terrestrial ecosystem model and validated using AsiaFlux data. *Agric For Meteorol* 148:738–747
- Kato T, Tang Y (2008) Spatial variability and major controlling factors of CO<sub>2</sub> sink strength in Asian terrestrial ecosystems: evidence from eddy covariance data. *Glob Change Biol* 14:2333–2348
- Kato T, Tang Y, Gu S, Cui X, Hirota M, Du M, Li Y, Zhao X, Oikawa T (2004) Carbon dioxide exchange between the atmosphere and an alpine meadow ecosystem on the Qinghai-Tibetan Plateau, China. *Agric For Meteorol* 124:121–134
- Kicklighter DW, Bondeau A, Schloss AL, Kaduk J, McGuire AD, the Participants of the Potsdam NPP Model Intercomparison (1999) Comparing global models of terrestrial net primary productivity (NPP): global pattern and differentiation by major biomes. *Glob Change Biol* 5:16–24
- Kim J, Verma SB, Clement RJ (1992) Carbon dioxide budget in temperate grassland ecosystem. *J Geophys Res* 97:6057–6063
- Klein JA, Harte J, Zhao XQ (2004) Experimental warming causes large and rapid species loss, damped by simulated grazing, on the Tibetan Plateau. *Ecol Lett* 7:1170–1179
- Knorr W, Prentice IC, House JI, Holland EA (2005) Long-term sensitivity of soil carbon turnover to warming. *Nature* 433:298–301
- Li W, Zhou X (eds) (1998) *Ecosystems of Qinghai-Xizang (Tibetan) Plateau and approach for their sustainable management. Series of studies on Qinghai-Xizang (Tibetan) Plateau*. Guangdong Science & Technology Press, Guangdong
- Loreau M, Hector A (2001) Partitioning selection and complementarity in biodiversity experiments. *Nature* 412:72–76
- Loreau M, Naeem S, Inchausti P (eds) (2002) *Biodiversity and ecosystem functioning synthesis and perspectives*. Oxford University Press, Oxford
- Lund CP, Riley WJ, Pierce LL, Field CB (1999) The effects of chamber pressurization on soil-surface CO<sub>2</sub> flux and the implications for NEE measurements under elevated CO<sub>2</sub>. *Glob Change Biol* 5:269–281
- Meharg AA, Killham K (1995) Loss of exudates from the roots of perennial ryegrass inoculated with a range of microorganisms. *Plant Soil* 170:345–349
- Nakano T, Nemoto M, Shinoda M (2008) Environmental controls on photosynthetic production and ecosystem respiration in semi-arid grasslands of Mongolia. *Agric For Meteorol* 148:1456–1466
- Raich JW, Schlesinger WH (1992) The global carbon dioxide flux in soil respiration and its relationship to vegetation and climate. *Tellus* 44B:81–90

- Risch AC, Frank DA (2006) Carbon dioxide fluxes in a spatially and temporally heterogeneous temperate grassland. *Oecologia* 147:291–302
- Scurlock JMO, Hall DO (1998) The global carbon sink: a grassland perspective. *Glob Change Biol* 4:229–233
- Scurlock JMO, Johnson K, Olson RJ (2002) Estimating net primary productivity from grassland biomass dynamics measurements. *Glob Change Biol* 8:736–753
- Shaver GR, Street LE, Rastetter EB, Van Wijk MT, Williams M (2007) Functional convergence in regulation of net CO<sub>2</sub> flux in heterogeneous tundra landscapes in Alaska and Sweden. *J Ecol* 95:802–817
- Sims PL, Risser PG (2000) Grasslands. p. 323–356. Grasslands. In: Barbour MG, Billings WG (eds) North American terrestrial vegetation, 2nd edn. Cambridge University Press, New York
- Sjögersten SR, van der Wal R, Woodin SJ (2006) Small-scale hydrological variation determines landscape CO<sub>2</sub> fluxes in the high arctic. *Biogeochemistry* 80:235–246
- Street LE, Shaver GR, Williams M, Van Wijk MT (2007) What is the relationship between changes in canopy leaf area and changes in photosynthetic CO<sub>2</sub> flux in arctic ecosystems? *J Ecol* 95:139–150
- Thornley MN, Johnson IR (1990) Plant and crop modeling; a mathematical approach to plant and crop physiology. Clarendon, Oxford
- Tilman D, Reich PB, Knops J, Wedin D, Mielke T, Lehman C (2001) Diversity and productivity in a long-term grassland experiment. *Science* 294:843–845
- Turner DP, Urbanski S, Bremer D, Wofsy SC, Meyers T, Gower ST, Gregory M (2003) A cross-biome comparison of daily light use efficiency for gross primary production. *Glob Change Biol* 9:383–395
- Uchida M, Kishimoto M, Muraoka H, Nakatsubo T, Kanda H, Koizumi H (2009) Seasonal shift in factors controlling net ecosystem production in a high Arctic terrestrial ecosystem *J Plant Res.* doi:10.1007/s10265-009-0260-6
- Van der Wal R (2006) Do herbivores cause habitat degradation or vegetation state transition? Evidence from the tundra. *Oikos* 114:177–186
- Vojtech E, Loreau M, Yachi S, Spehn EM, Hector A (2008) Light partitioning in experimental grass communities. *Oikos* 117:1351–1361
- Wang W, Ohse K, Liu J, Mo W, Oikawa T (2005) Contribution of root respiration to soil respiration in a C3/C4 mixed grassland. *J Biosci* 30:507–514
- Wilsey BJ, Parent G, Roulet NT, Moore TR, Potvin C (2002) Tropical pasture carbon cycling: relationships between C source/sink strength, above-ground biomass and grazing. *Ecol Lett* 5:367–376
- Xu LK, Baldocchi DD (2004) Seasonal variation in carbon dioxide exchange over a Mediterranean annual grassland in California. *Agric For Meteorol* 123:79–96
- Zhang P, Tang Y, Hirota M, Yamamoto A, Mariko S (2009) Use of a regression method to partition sources of ecosystem respiration in an alpine meadow. *Soil Biol Biochem* 41:663–670
- Zhao L, Li Y, Xu S, Zhou H, Gu S, Yu G, Zhao X (2006) Diurnal, seasonal and annual variation in net ecosystem CO<sub>2</sub> exchange of an alpine shrubland on Qinghai-Tibetan plateau. *Glob Change Biol* 12:1940–1953